



## Marangoni flow in floating half zone of molten tin



Kai Li <sup>a,\*</sup>, Satoshi Matsumoto <sup>b</sup>, Nobuyuki Imaishi <sup>c,\*</sup>, Wen-Rui Hu <sup>a</sup>

<sup>a</sup> Key Laboratory of Microgravity, Institute of Mechanics, Chinese Academy of Sciences, Beijing 100190, China

<sup>b</sup> Institute of Space and Astronautical Science, Japan Aerospace Exploration Agency, 2-1-1 Sengen, Tsukuba, Japan

<sup>c</sup> Institute for Materials Chemistry and Engineering, Kyushu University, 6-1 Kasuga Koen, Kasuga 816-8580, Japan

### ARTICLE INFO

#### Article history:

Received 20 January 2014

Received in revised form 20 November 2014

Accepted 3 December 2014

Available online 8 January 2015

#### Keywords:

Marangoni flow

Flow instabilities

Deformed half zone

Buoyancy

### ABSTRACT

Gravity affects the stability of Marangoni flow in floating half zone of low-Pr fluids through two different factors, i.e., the buoyancy and the static deformation of the free surface shape. In the present study, influence of these two factors are evaluated by unsteady three-dimensional (3D) simulations for a realistic model of floating half zone of molten tin ( $Pr = 0.009$ ) with an aspect ratio  $As = 2.0$  under a ramped temperature difference (1.19 K/min) between the top and bottom ends of two iron supporting rods. The corresponding first critical conditions for the onset of 3D asymmetric non-oscillatory flows and the second critical conditions for the onset of 3D oscillatory flows are determined. Simulation results indicate that the free surface deformation is the most influential factor for the critical conditions of the flow transitions. Buoyancy is less influential to the flow transitions. However, buoyancy causes multiple step transitions between different 3D asymmetric non-oscillatory flow modes.

© 2014 Elsevier Ltd. All rights reserved.

### 1. Introduction

The stability of the surface tension driven flow (Marangoni flow) in floating half zone of low-Pr fluids has been the subject of extensive research for decades. It was motivated by the experimental fact that an oscillatory Marangoni flow in floating zone configurations may be responsible for striations in crystals grown using a partially covered floating zone method [1] and floating zone Si crystal grown in space [2]. Since the first prediction through the three-dimensional (3D) numerical simulation by Rupp et al. [3], numerous linear stability analyses (LSA), e.g. [4–7], and nonlinear numerical simulations, e.g. [5,6], have proved that Marangoni flow in floating half zone (noted as FHZ, hereafter) of low-Pr fluids becomes oscillatory through a two step bifurcations: the first bifurcation from an axisymmetric non-oscillatory flow to a 3D asymmetric non-oscillatory flow occurs at a certain Reynolds number (the first critical Reynolds number:  $Re_{c1}$ ) and the second bifurcation to a 3D oscillatory flow occurs at much larger Reynolds number (the second critical Reynolds number:  $Re_{c2}$ ). Moreover, these 3D flows in FHZ of low-Pr fluids are caused by hydrodynamic instability mechanism [4,5], rather than the hydrothermal wave instability mechanism [8] which is widely known as the cause of the oscillatory 3D flow in FHZs of moderate-Pr and high-Pr fluids

[4,5]. Velten et al. [9] experimentally found that the critical Reynolds number for the onset of oscillatory flow in FHZ of moderate-Pr fluid heated from bottom is larger than that obtained when heated from top. Wanschura et al. [10] studied the effect of gravity on the Marangoni flow in FHZ by linear stability analysis and confirmed the counterintuitive experimental fact found by Velten et al. [9]. However, the mechanism was not clearly explained. Also their analysis predicts this apparently contradictory stabilizing effect of buoyancy may occur in FHZ of low-Pr fluid. These theoretical and numerical predictions are not yet validated by comparing with reliable experimental results. There are many experimental reports on the oscillation frequency and flow patterns of oscillatory flow in FHZ of low-Pr fluids such as molten silicon [11] and molten silver [12]. However, these high temperature experiments are unsuitable for measuring a small temperature difference to detect the critical conditions. There are some studies on oscillatory Marangoni flow in FHZ at lower temperatures, e.g. Han et al. with mercury [13] and Yang and Kou with molten tin [14]. According to these experiments,  $Ma_{c2}$  for a transition to oscillatory flow ranges between 200 and 900 and  $Ma_{c1}$  was not detected. JAXA started a series of on-ground experiments, e.g. [15–17], searching both flow transition conditions,  $Re_{c1}$  and  $Re_{c2}$  in FHZ of molten tin ( $Pr = 0.009$ ). Correspondingly, a series of numerical simulations on Marangoni flow in FHZ of molten tin have been conducted based on a simple FHZ model such as a cylindrical FHZ held between two circular heating/cooling disks [18,19] or a cylindrical FHZ held between two iron rods [20,21]. In these simulations, effects of the aspect

\* Corresponding authors.

E-mail addresses: [likai@imech.ac.cn](mailto:likai@imech.ac.cn) (K. Li), [imaishi@cm.kyushu-u.ac.jp](mailto:imaishi@cm.kyushu-u.ac.jp) (N. Imaishi).

ratio of FHZ on the flow instability under microgravity condition were systematically studied. Li et al. [21] studied the effect of ramping rate of temperature difference by numerical simulations. It was confirmed that the larger temperature ramping retards the flow transitions which raised the experimentally determined  $Re_{c1}$  and  $Re_{c2}$ . However, buoyancy and free surface deformation caused by the gravity were not considered in these studies.

For a quantitative comparison of the critical conditions determined through numerical simulations to the results through on-ground experiments, numerical simulations must include all gravity-related factors, i.e. static deformation of free surface and the buoyancy. Many numerical studies on flow instabilities have been done for non-cylindrical FHZ under microgravity, i.e., the effect of liquid volume. These works were reviewed and benchmark-tested by Shevtsova [22]. To our knowledge, there are only a few linear stability analyses and numerical simulations on the instabilities of buoyant-Marangoni convection in gravitationary deformed FHZ of low-Pr fluids. Nienheuser and Kuhlmann [23] conducted a linear stability analysis of axisymmetric Marangoni flow in FHZ with non-cylindrical surfaces for  $Pr = 0.02$  and  $Pr = 4$ . Kuhlmann et al. [24] conducted linear stability analysis of axisymmetric flow in gravitationary deformed FHZ with unity aspect ratio for  $Pr = 0 \sim 0.04$ . In the papers, they provided a plot of  $Re_{c1}$  as a function of Bond number and heating direction for  $Pr = 0.023$ . Lappa et al. [25] studied stability limit of Marangoni flow in deformed FHZ of silicon ( $Pr = 0.01$ ) and gallium ( $Pr = 0.04$ ) by comparing with their own results for cylindrical FHZ with an aspect ratio  $As = 2.0$ . These works treated the static deformation of the surface. Shevtsova [22] included  $Re_{c1}$  for gravitationary deformed FHZ in the benchmark topics but  $Re_{c2}$  was not tested. However, the combined effects of buoyancy and free surface deformation on the Marangoni flow in FHZ of low-Pr fluids under earth gravity (1G) are yet not fully discerned. It should be noted that Kuhlmann and Nienheuser et al. [23] studied the effect of dynamic surface deformation on the instability and the amplitudes of dynamic deformations are so small that would not cause significant effects.

In the present study, the combined effects of buoyancy and static surface deformation on time evolution of Marangoni flow and flow transition processes in a FHZ of  $Pr = 0.009$  with  $As = 2.0$  under a ramped temperature difference are studied by numerical simulations based on a realistic FHZ model. A ramp rate of 1.19 K/min is assumed for the time-dependent temperature difference between both ends of the two supporting iron rods. In order to distinguish effects of free surface deformation and buoyancy, behavior of FHZ under special situations, i.e., cylindrical FHZ with buoyancy ( $Bo \neq 0$ ,  $Gr \neq 0$ ) and deformed FHZ without buoyancy ( $Bo \neq 0$ ,  $Gr = 0$ ) were also studied using two imaginary fluids. These imaginary fluids, Fluid A and Fluid B, are assumed to have the same thermophysical properties of molten tin except for either surface tension (quite large surface tension) or thermal expansion coefficient (no thermal expansion), respectively.

## 2. Model and methods

The schematics of a realistic FHZ of molten tin are shown in Fig. 1. The melt zone of molten tin is supported between two iron rods. The melt is assumed to be an incompressible Newtonian fluid and further adopted the Boussinesq assumption except for the temperature dependencies of density and surface tension. Thermophysical properties of molten tin and iron rod are shown in Table 1 together with the two imaginary fluids (Fluid A and Fluid B). A cylindrical coordinate system ( $R, \theta, Z$ ) is adopted with the origin located at the center of the lower melt/rod interface. The radius of the supporting rod is denoted as  $a$ . The melt zone length and

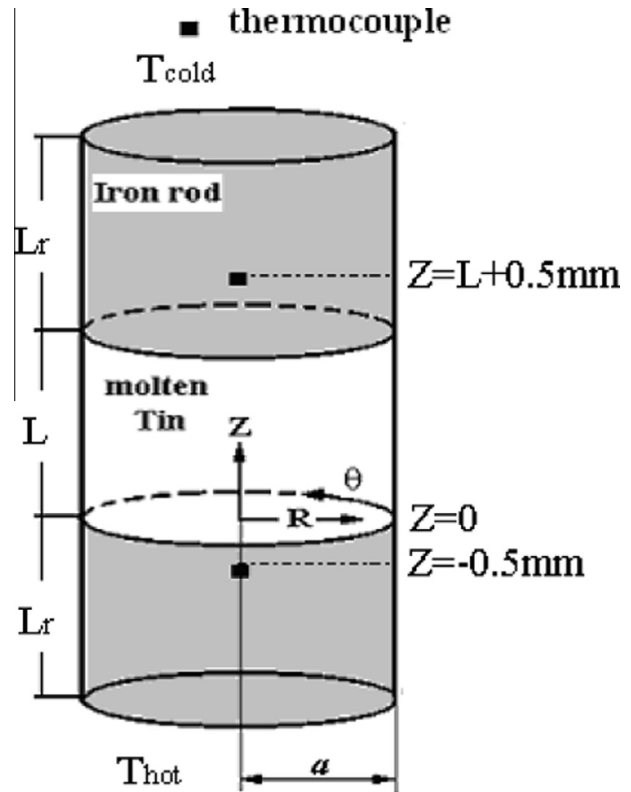


Fig. 1. Schematics of a realistic floating half zone (FHZ) model.

Table 1  
Thermophysical properties.

	Molten tin	Fluid A	Fluid B	Iron
$\rho$ (kg/m <sup>3</sup> )	6793	6793	6793	7700
$k$ (W/mK)	35.44	35.44	35.44	20.0
$C_p$ (J/kgK)	242	242	242	460
$\nu$ (m <sup>2</sup> /s)	$1.94 \times 10^{-7}$	$1.94 \times 10^{-7}$	$1.94 \times 10^{-7}$	–
$\sigma$ (N/m)	0.5	$\gg 1$	0.5	–
$\sigma_T$ (N/mK)	$-1.3 \times 10^{-4}$	$-1.3 \times 10^{-4}$	$-1.3 \times 10^{-4}$	–
$\beta$ (1/K)	$1.3 \times 10^{-4}$	$1.3 \times 10^{-4}$	0	–

iron rod length are denoted  $L$  and  $L_r$  with the aspect ratios  $As = L/a$  and  $As_r = L_r/a$ , respectively. In the present study, ( $a = 3.0$  mm,  $As = As_r = 2.0$ ) is adopted. The fluid is initially motionless and kept at a uniform temperature  $T_0 = 703.6$  K, and subsequently linearly increasing temperature difference were applied on the top end and bottom end of the supporting iron rods ( $T_H$  and  $T_C$ ). Based on the experimental average ramping rate 0.34 K/min measured through the thermocouples located at 0.5 mm apart from the melt/rod interfaces (see Fig. 1) during one of the experiments conducted at JAXA [15], the ramping rate of the temperature difference is determined as  $d(T_H - T_C)/dt = 1.19$  K/min by the pure steady conduction model [19,20]. Therefore, the time-dependent temperatures at the ends of the supporting rods are  $T_H = 703.6 + 0.009917 t$  [K] and  $T_C = 703.6 - 0.009917 t$  [K], respectively.

The fundamental equations are expressed as follows:

In the melt zone:

$$\nabla \cdot \mathbf{U} = 0 \quad (2.1)$$

$$\frac{\partial \mathbf{U}}{\partial t} + \mathbf{U} \cdot \nabla \mathbf{U} = \frac{1}{\rho} \nabla p + \nu \nabla^2 \mathbf{U} - \beta g (T - T_0) \mathbf{e}_z \quad (2.2)$$

Download English Version:

<https://daneshyari.com/en/article/657210>

Download Persian Version:

<https://daneshyari.com/article/657210>

[Daneshyari.com](https://daneshyari.com)